Equilibria Between Gas and Liquid Phases for Concentrated Aqueous Solutions of Nitric Acid

Fanny Balbaud,*[a] Gérard Sanchez,[a] Gérard Santarini,[a] and Gérard Picard[b]

Keywords: Nitric acid / Nitrogen oxides / Electrochemistry / Thermodynamics

Calculated diagrams, representing chemical and electrochemical properties of concentrated aqueous nitric acid mixtures, have been drawn for temperatures of 25 °C and 100 °C using vapor pressures and thermochemical data of related gaseous species. Electrochemical measurements have permitted the establishment of an experimental potential scale (referenced to the saturated mercurous sulfate electrode at 25 °C) incorporated in the diagram at 100 °C. These measurements also allowed the determination of the Gibbs free energy of formation of dissolved nitrous acid for various nitric acid solutions at 100 °C, leading to a value of $\Delta G_f(HNO_2) = –36.31$ kJ mol^{-1}, for the whole nitric acid concentration range.

Introduction

Nuclear fuel reprocessing is achieved in France using nitric acid as the dissolution reaction medium. Nitric acid acts as an oxidizing agent and is currently used over a large range of concentration, e.g. 1 mol L^{-1} to 14.4 mol L^{-1}, and temperature, from room temperature to boiling point (at atmospheric pressure). The corrosive nature of these nitric mixtures leads to the use of corrosion-resistant materials such as austenitic stainless steels and zirconium. Corrosion studies of selected materials have previously been performed in the CEA-CEREM laboratories in an attempt to answer many practical industrial problems.[1,2] A more fundamental study of corrosion in these mixtures was undertaken some years ago[3] and showed the necessity of investigating thoroughly the corrosive nature of the reaction medium as had been performed for fused sodium nitrate−nitrite mixtures.[4a,4b]

The main objective of the study presented in this paper is to build up a synthetic thermodynamic representation of the chemical properties of concentrated nitric media. This representation connects with the Pourbaix diagram[5] for solutions of positive pH and gives a picture of the medium for more concentrated solutions. The construction of this thermodynamic representation involves knowledge of the thermochemical data of all the species present in the medium. As the value of the Gibbs free energy of formation of nitrous acid (one of the major soluble nitrogenous species apart from nitric acid) in nitric acid at 100°C appeared to be uncertain, electrochemical measurements were performed to determine this datum. These measurements also allowed the establishment of an experimental potential scale for the diagram.

Analysis of Available Literature Data and Graphic Representation of the Chemical Properties of Nitric Media

Nitric acid and water vapor pressures for acid concentrations varying from 0% to 95% and temperatures from 0°C to 140°C may be found from an analysis of literature data [Tables 1 and 2; all the pressures are given in bar (1 bar = 10^5 Pa)].[6−15]

The major interest in considering the gaseous forms of the different substances is that it makes possible the use of thermochemical data associated with the gaseous pure substances instead of those of soluble species which are generally not known with a great accuracy for concentrated media. Thermochemical data used for the calculations are presented in Table 3.[16−19]

Principle of the Construction of a Potential−Acidity-Type Diagram

All species are gaseous, including water and nitric acid, and thermochemical data used are those of pure substances under a pressure of 1 bar. The diagram was drawn using the coordinates $\log(P_{O_2}) = f[-\log(P_{HNO_3})$ or pH]. The curves represent the calculated values of the oxygen pressure for which the partial pressures of the various gaseous species are equal to 1 bar and 0.1 bar. For pH < 0, the x axis is plotted as $-\log(P_{HNO_3})$; this parameter allows the scale to be expanded and avoids the problems of proton activity in a concentrated medium. For pH > 0 the classical pH scale is used and the representation becomes equivalent to a Pourbaix diagram. The y axis is in $\log(P_{O_2})$. This choice allows the exclusive use of gaseous species, without making any approximation concerning the nitric acid dissociation

---

[a] CEA-CEREM, Service de la Corrosion, d'Electrochimie et de Chimie des Fluides,
B. P. 6, F-92265 Fontenay-aux-Roses Cedex, France
E-mail: fbalbaud@teaser.fr and santarini@cyborg.cea.fr
[b] Laboratoire d'Electrochimie et de Chimie Analytique (UMR 7575 du C.N.R.S.), Ecole Nationale Supérieure de Chimie de Paris,
11 rue Pierre et Marie Curie, F-75231 Paris Cedex 05, France
E-mail: picard@ext.jussieu.fr

1434−1948/99/0202−0277 $ 17.50+.50/0

Table 1. Vapor pressures of water as a function of temperature and nitric acid concentration [wt-%][6−15]

T [°C]	20%	30%	40%	50%	60%	70%	80%	90%
0	0.0052	$4.44{\cdot}10^{-3}$	$3.72{\cdot}10^{-3}$	$2.34{\cdot}10^{-3}$	$2.07{\cdot}10^{-3}$	$1.32{\cdot}10^{-3}$	$5.51{\cdot}10^{-4}$	$1.58{\cdot}10^{-4}$
10	0.0104	$8.77{\cdot}10^{-3}$	$7.20{\cdot}10^{-3}$	$5.17{\cdot}10^{-3}$	$4.10{\cdot}10^{-3}$	$2.67{\cdot}10^{-3}$	$1.31{\cdot}10^{-3}$	$2.70{\cdot}10^{-4}$
20	0.0196	0.0165	0.0133	$9.72{\cdot}10^{-3}$	$7.48{\cdot}10^{-3}$	$5.13{\cdot}10^{-3}$	$2.90{\cdot}10^{-3}$	$8.54{\cdot}10^{-4}$
30	0.0355	0.0297	0.0238	0.0176	0.0135	$9.37{\cdot}10^{-3}$	$5.68{\cdot}10^{-3}$	$2.16{\cdot}10^{-3}$
40	0.0616	0.0514	0.0409	0.0307	0.0237	0.0164	0.0103	$4.27{\cdot}10^{-3}$
50	0.1031	0.0859	0.0680	0.0519	0.0402	0.0278	0.0174	$7.15{\cdot}10^{-3}$
60	0.1669	0.1388	0.1098	0.0849	0.0663	0.0459	0.0282	0.0111
70	0.2621	0.2180	0.1725	0.1350	0.1062	0.0738	0.0448	0.0170
80	0.4003	0.3333	0.2643	0.2094	0.1657	0.1157	0.0704	0.0283
90	0.5964	0.4973	0.3958	0.3174	0.2524	0.1767	0.1076	0.0464
100	0.8680	0.7256	0.5800	0.4705	0.3760	0.2622	0.1597	0.0738
110	1.2358	1.0351	0.8329	0.6833	0.5487	0.3799	0.2290	0.1075
120	1.7214	1.4449	1.1730	0.9735	0.7845	0.5408	0.3257	0.1319

Table 2. Vapor pressures of nitric acid as a function of temperature and nitric acid concentration [wt-%][6−15]

T [°C]	20%	30%	40%	50%	60%	70%	80%	90%
0	$4.17{\cdot}10^{-6}$	$5.21{\cdot}10^{-6}$	$8.36{\cdot}10^{-6}$	$1.52{\cdot}10^{-5}$	$9.79{\cdot}10^{-5}$	$1.17{\cdot}10^{-3}$	$3.12{\cdot}10^{-3}$	$8.13{\cdot}10^{-3}$
10	$8.91{\cdot}10^{-6}$	$1.16{\cdot}10^{-5}$	$2.80{\cdot}10^{-5}$	$1.02{\cdot}10^{-4}$	$3.48{\cdot}10^{-4}$	$2.32{\cdot}10^{-3}$	$6.18{\cdot}10^{-3}$	0.0177
20	$1.86{\cdot}10^{-5}$	$2.89{\cdot}10^{-5}$	$7.66{\cdot}10^{-5}$	$2.71{\cdot}10^{-4}$	$8.78{\cdot}10^{-4}$	$4.39{\cdot}10^{-3}$	0.0115	0.0347
30	$3.46{\cdot}10^{-5}$	$6.67{\cdot}10^{-5}$	$1.82{\cdot}10^{-4}$	$5.85{\cdot}10^{-4}$	$1.86{\cdot}10^{-3}$	$8.02{\cdot}10^{-3}$	0.0207	0.0632
40	$6.18{\cdot}10^{-5}$	$1.47{\cdot}10^{-4}$	$3.99{\cdot}10^{-4}$	$1.18{\cdot}10^{-3}$	$3.63{\cdot}10^{-3}$	0.0141	0.0359	0.1081
50	$1.09{\cdot}10^{-4}$	$3.10{\cdot}10^{-4}$	$8.19{\cdot}10^{-4}$	$2.28{\cdot}10^{-3}$	$6.61{\cdot}10^{-3}$	0.0239	0.0603	0.1761
60	$2.00{\cdot}10^{-4}$	$6.37{\cdot}10^{-4}$	$1.63{\cdot}10^{-3}$	$4.24{\cdot}10^{-3}$	0.0115	0.0390	0.0977	0.2739
70	$3.67{\cdot}10^{-4}$	$1.25{\cdot}10^{-3}$	$3.09{\cdot}10^{-3}$	$7.60{\cdot}10^{-3}$	0.0193	0.0613	0.1527	0.4089
80	$6.66{\cdot}10^{-4}$	$2.34{\cdot}10^{-3}$	$5.64{\cdot}10^{-3}$	0.0131	0.0318	0.0939	0.2305	0.5862
90	$1.22{\cdot}10^{-3}$	$4.20{\cdot}10^{-3}$	$9.94{\cdot}10^{-3}$	0.0218	0.0506	0.1405	0.3389	0.8135
100	$2.45{\cdot}10^{-3}$	$7.33{\cdot}10^{-3}$	0.0169	0.0354	0.0787	0.2069	0.4869	1.098
110	$5.81{\cdot}10^{-3}$	0.0140	0.0282	0.0560	0.1196	0.2997	0.6871	1.450
120	0.0158	0.0287	0.0471	0.0870	0.1793	0.4249	0.9465	1.897

Table 3. Literature values for the Gibbs free energy of formation used in the thermochemical calculations at 25°C and 100°C;[16−19] dissociation constant of nitric acid [$HNO_3(g) \rightleftharpoons H^+ + NO_3^-$]: $K = 3.22 \cdot 10^6$ mol^2 L^{-2} bar^{-1} at 25°C[18]$K = 4.874 \cdot 10^3$ mol^2 L^{-2} bar^{-1} at 100°C[19]

	$\Delta G^0{}_f$/kJ mol^{-1}; T = 25°C	$\Delta G^0{}_f$/kJ mol^{-1}; T = 100°C
$HNO_3(g)$	−73.964[16]	−58.634[17]
$NO_2(g)$	51.262[16]	55.872[17]
$N_2O_4(g)$	97.788[16]	120.020[17]
$NO(g)$	86.599[16]	85.621[17]
$N_2O(g)$	104.172[16]	109.768[17]
$H_2O(g)$	−228.620[16]	−225.138[17]

or the proton activity. The partial pressures of the gases are considered to be equal to their fugacities.

Calculated Diagrams at 25°C and 100°C (Involving Only Gaseous Species)

The following equilibria were considered in order to represent the variations of oxygen pressure for the different gases:

$$2\ HNO_3 \rightleftharpoons N_2 + \frac{5}{2}O_2 + H_2O \qquad (a)$$

$$2\ HNO_3 \rightleftharpoons N_2O + 2O_2 + H_2O \qquad (b)$$

$$2\ HNO_3 \rightleftharpoons 2\ NO + \frac{3}{2}O_2 + H_2O \qquad (c)$$

$$\text{at 100°C: } 2\ HNO_3 \rightleftharpoons 2\ NO_2 + \frac{1}{2}O_2 + H_2O \qquad (d)$$

$$\text{at 25°C: } 2\ HNO_3 \rightleftharpoons N_2O_4 + \frac{1}{2}O_2 + H_2O \qquad (e)$$

At 25°C, the dimer N_2O_4 is the predominant form whilst at 100°C the monomer NO_2 is the predominant form for pressures of 1 bar and 0.1 bar.

For each reaction, the equilibrium constant can be written as a function of the pressures of the different gases. For reaction (a), the equilibrium constant may be expressed as:

$$K_a = \frac{P_{N_2} P_{O_2}^{5/2} P_{H_2O}}{P_{HNO_3}^2}$$

For a given temperature, the equilibrium constant K_a can be calculated, as the Gibbs free energies of formation of the different gases are known in the literature. The variation of the logarithm of the oxygen pressure can then be expressed as:

$$\log P_{O_2} = \frac{2}{5}\log K_a - \frac{2}{5}\log P_{H_2O} - \frac{4}{5}\log P_{HNO_3} - \frac{2}{5}\log_{N_2} \qquad (7)$$

For given nitric acid concentration and temperature, the nitric acid and water vapor pressures are known and it is

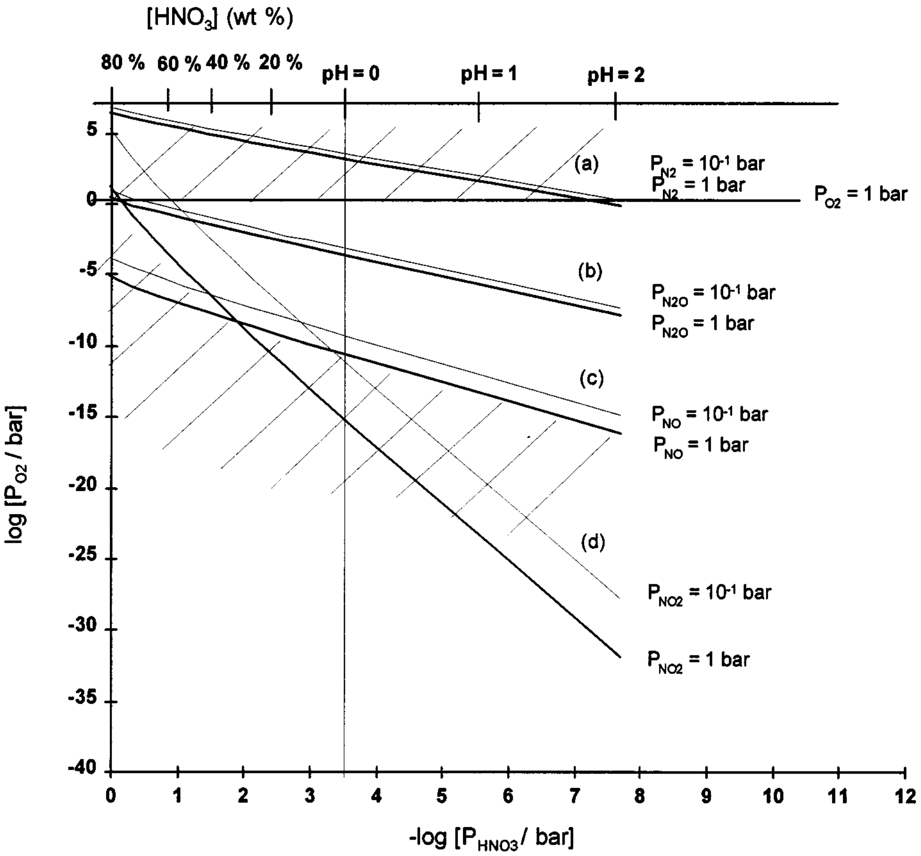

Figure 1. Calculated thermochemical diagram of nitric acid at 100°C involving gaseous species − stability domain of nitric acid under a pressure of 1 bar

therefore possible to determine the variation of the oxygen pressure with the nitric acid vapor pressure, for a given nitrogen pressure. For the other equilibria, the same calculation method may be used.

Theoretical representations in [log (P_{O_2})] − [−log (P_{HNO_3})] were calculated from the thermochemical data available in the literature at 100°C and 25°C (Figures 1 and 2).

Experimental Results and Discussion

In order to determine the missing datum of the free energy of formation of nitrous acid in nitric acid solutions at 100°C, potentiometric measurements were performed. All the measurements were referenced to the saturated mercurous sulfate electrode at 25°C (SSE).

Potentiometric Study; Determination of the Standard Potentials of the HNO_3/HNO_2 Electrochemical System at 100°C

To determine the standard potential of the HNO_3/HNO_2 system, the potential of the platinum electrode was measured at 100°C as a function of the concentration of nitrite (nitrous acid) in different nitric acid solutions (Figure 3). Initially, with no addition of nitrite, the concentration of nitrous acid in the nitric acid solution was approximately of 10^{-6} mol L^{-1}.

Nitrite ions were added as $NaNO_2$ in a 2.3 mol L^{-1} aqueous solution. In concentrated nitric acid, nitrite ions exist in the form of nitrous acid, HNO_2. During the potential measurements, the concentration of nitrous acid in nitric acid solution was considered equal to the concentration of nitrite added. This assumption was verified by analyzing the solutions for an expected value of 10^{-3} mol L^{-1}. The results obtained are given in Table 4 and show a good agreement. The following reduction reaction was considered:

$$HNO_{3(g)} + 2\,H^{+}_{(aq.)} + 2\bar{e} \rightleftharpoons HNO_{2(aq)} + H_2O_{(g)} \qquad (1)$$

For this reaction, the Nernst equation can be written as:

$$E = E_1^0 + \frac{RT}{2F}\ln\left(\frac{P_{HNO_3}[H^+]^2}{P_{H_2O}[HNO_2]}\right)$$

The experimental measurements of the potential of the platinum electrode, as a function of the nitrous acid concentration, lead to the determination of the apparent standard potential $E_1^{0'}$ of the HNO_3/HNO_2 system. This apparent standard potential is the potential measured for a nitrous acid concentration of 1 mol L^{-1}, the concentrations of the other species being fixed by the solution. It can be expressed as:

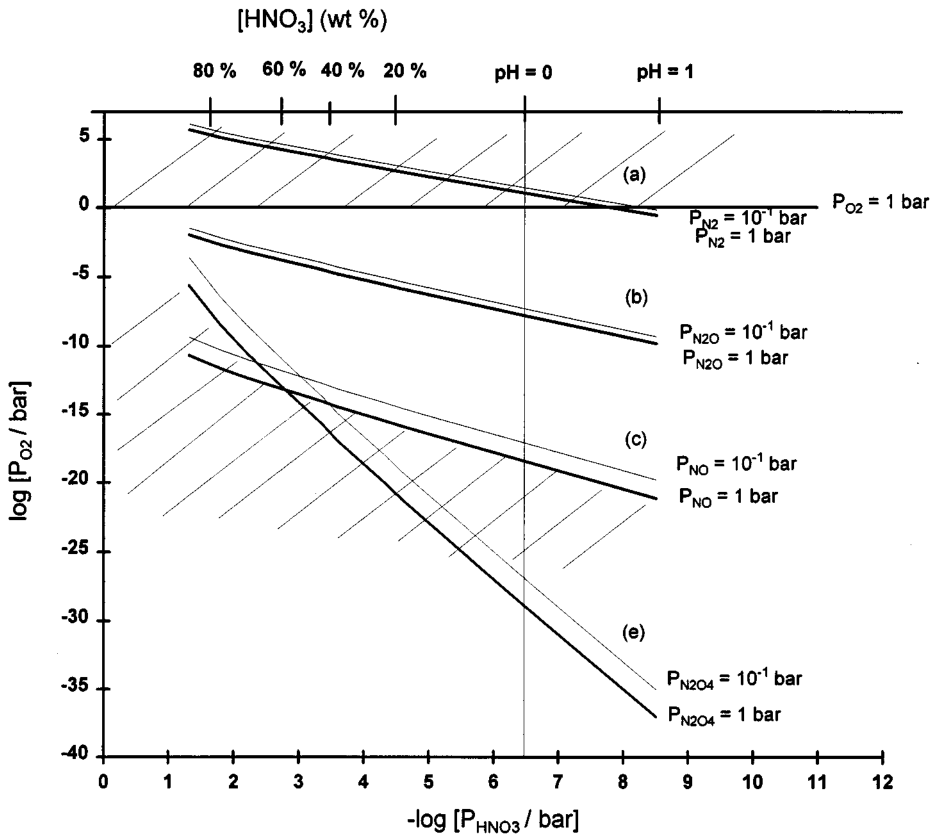

Figure 2. Calculated thermochemical diagram of nitric acid at 25°C involving gaseous species − stability domain of nitric acid under a pressure of 1 bar

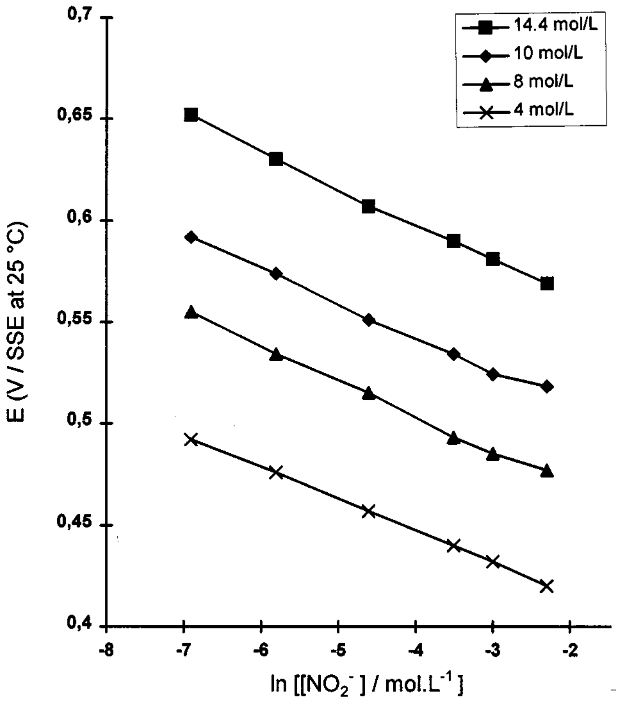

Figure 3. Potential of the platinum working electrode as a function of the concentration of nitrite added in solution and of the nitric acid concentration at 100°C

Table 4. Experimental measurement of the nitrite (nitrous acid) concentration in solution as a function of the nitric acid concentration; $[HNO_2]_{added} = 10^{-3}$ mol L^{-1} (theoretical concentration)

$[HNO_3]$/mol L^{-1}	$[HNO_2]$/mol L^{-1} measured in solution
4	$8.9 \cdot 10^{-4}$
8	$8.7 \cdot 10^{-4}$
10	$9.6 \cdot 10^{-4}$
14.4	$1.2 \cdot 10^{-3}$

$$E_1^{0'} = E_1^0 + \frac{RT}{2F}\ln\left(\frac{P_{HNO_3}[H^+]^2}{P_{H_2O}}\right)$$

The potential can then be written as:

$$E = E_1^{0'} - \frac{RT}{2F}\ln[HNO_2]$$

The variations of the potential of the platinum electrode, as a function of the nitrous acid concentration, are represented in Figure 3 for four nitric acid solutions of concentrations of 4 mol L^{-1}, 8 mol L^{-1}, 10 mol L^{-1}, and 14.4 mol L^{-1}. The experimental slope obtained with the linear regression analysis varies from 0.0178 for 14.4 mol L^{-1} to 0.0156 for 4 mol L^{-1}. The theoretical slope being equal to 0.0161, it can be inferred that the HNO_3/HNO_2 system follows the Nernst law.

Table 5 gives the experimental apparent standard potentials for the different solutions, $E_1^{0\prime}$. The values were determined by a linear regression analysis performed by fixing the value of the slope at the Nernst value.

Table 5. Experimental apparent standard potentials of HNO_3/HNO_2 and HNO_3/NO_2 systems as a function of nitric acid concentration at 100°C

$[HNO_3]$ [mol L^{-1}]	$E^0_{app.}(HNO_3/HNO_2)$ (V/SSE) = $E_1^{0\prime}$	$E^0_{app.}(HNO_3/NO_2)$ (V/SSE) = $E_2^{0\prime}$
14.4	0.535±5 mV	0.615±2 mV
10	0.478±3 mV	–
8	0.440±4 mV	0.474±4 mV
4	0.383±2 mV	0.391±5 mV

Determination of the Standard Potentials of the HNO_3/NO_2 Electrochemical System at 100°C

To determine the standard potential of the HNO_3/NO_2 system, the potential of the platinum electrode was measured at 100°C as a function of the nitrogen dioxide pressure (Figure 4). The nitrogen dioxide pressure was fixed and controlled by a continuous flow of NO_2 in the reactor. The measurement was performed after stabilization of the potential. No measurement was performed for a nitric acid concentration of 10 mol L^{-1}.

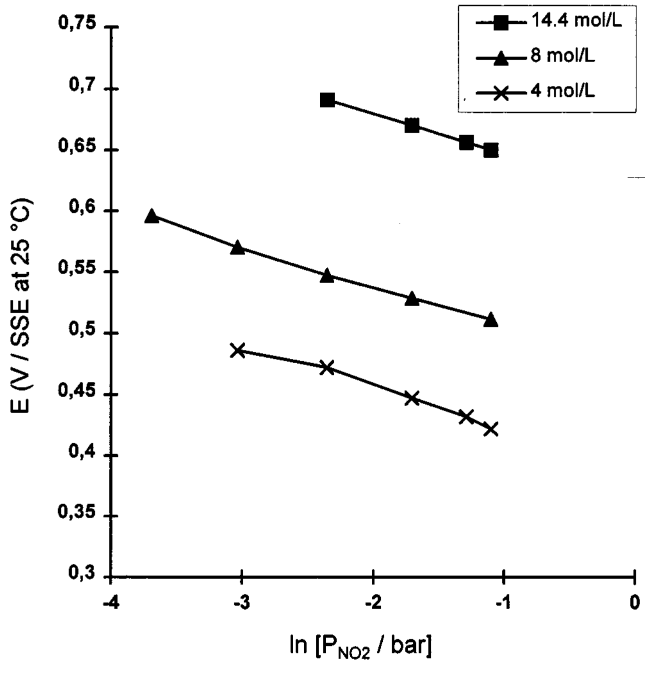

Figure 4. Potential of the platinum working electrode as a function of the nitrogen dioxide pressure and of the nitric acid concentration at 100°C

The following reaction was considered:

$$HNO_{3(g)} + H^+_{(aq.)} + \bar{e} \rightleftharpoons NO_{2(g)} + H_2O_{(g)} \qquad (2)$$

According to this reaction, the Nernst equation can be written:

$$E = E_2^0 + \frac{RT}{F}\ln\left(\frac{P_{HNO_3}[H^+]}{P_{H_2O}\,P_{NO_2}}\right)$$

As previously, it is possible to define an apparent standard potential:

$$E_2^{0\prime} = E_2^0 + \frac{RT}{F}\ln\left(\frac{P_{HNO_3}[H^+]}{P_{H_2O}}\right)$$

Then:

$$E = E_2^{0\prime} - \frac{RT}{F}\ln(P_{NO_2})$$

The variations of the potential as a function of the nitrogen dioxide pressure are represented in Figure 4 for three nitric acid concentrations, 4 mol L^{-1}, 8 mol L^{-1}, and 14.4 mol L^{-1}. The experimental slope varies from 0.0325 for 8 mol L^{-1} to 0.0330 for 4 mol L^{-1}. In this case the theoretical slope is equal to 0.0321; therefore HNO_3/NO_2 shows Nernst-like behavior. The values of the apparent standard potentials of HNO_3/NO_2 are reported in Table 5.

Calculation of the Gibbs Free Energy of Formation of Nitrous Acid at 100°C

Combining the expressions of the equilibrium potential obtained for the HNO_3/HNO_2 and for the HNO_3/NO_2 systems, the following equation can be written:

$$E_2^{0\prime} = E_1^{0\prime} + \frac{RT}{2F}\ln\left(\frac{P^2_{NO_2}}{[HNO_2]}\right)$$

The ratio of the square nitrogen dioxide pressure to the nitrous acid concentration (right term) is linked to the equilibrium constant, K_3, of the following reaction, by the ratio of the partial pressure of nitric acid to the partial pressure of water:

$$HNO_{3(g)} + HNO_{2(aq.)} \rightleftharpoons 2\,NO_{2(g)} + H_2O_{(g)} \qquad (3)$$

Therefore, the constant K_3, for a given nitric acid solution (concentration and temperature fixed), can be deduced from the apparent standard potentials according to the expression:

$$K_3 = \frac{P_{H_2O}}{P_{HNO_3}}\exp\left(\frac{2F}{RT}(E_2^{0\prime} - E_1^{0\prime})\right)$$

Experimentally, the standard apparent potentials of the systems HNO_3/HNO_2 and HNO_3/NO_2 have been determined for nitric acid concentrations of 4 mol L^{-1}, 8 mol L^{-1}, and 14.4 mol L^{-1}. Therefore the constant K_3 for these concentrations can be easily calculated, without making any assumption of the proton activity or of the reference system used. Moreover, with this calculation method, uncertainties in the potential measurements, linked to an eventual liquid-junction potential, are avoided if this potential is supposed to be constant for all the measurements.

As the Gibbs free energies of formation of gaseous nitric acid, gaseous water and nitrogen dioxide are known, and as for a given nitric acid solution, the partial pressures of water and nitric acid are also known, it is possible to calculate the Gibbs free energy of formation of dissolved nitrous acid in 4 mol L^{-1}, 8 mol L^{-1}, and 14.4 mol L^{-1} solutions. The results are reported in Table 6 in which the three values obtained from the calculations on the apparent standard potentials are given with all the figures obtained. The three values are quite close and therefore a mean value of the Gibbs free energy of formation of nitrous acid at 100°C was determined as $\Delta G_f(HNO_2) = -36.3 \pm 1$ kJ mol^{-1}.

This value is considered constant for the whole nitric acid concentration range. The error of 1 kJ mol^{-1} corresponds to a potential measurement error of ± 5 mV. In Table 6, two literature values corresponding to the Gibbs free energy of formation of dissolved nitrous acid in water at 100°C, are reported.[20,21] These values are quite different and the experimental datum determined above is intermediate between them.

Table 6. Experimental values of the free energy of formation of nitrous acid in various nitric acid solutions (results obtained by a calculation made with the experimental standard potentials); literature values in water at 100°C[20,21]

$[HNO_3]$ [mol L^{-1}]	$\Delta G_f(HNO_2)$ at 100°C [kJ mol^{-1}]
4	−35.703
8	−37.230
14.4	−36.110
Water (literature data)	−38.456[20] and −32.617[21]

Joint Use of Thermochemical and Potentiometric Data for Establishing an Improved Potential−Acidity Diagram for Nitric Media

Calculated Diagrams at 25°C and 100°C

The curves on the diagrams (Figures 1 and 2) represent the calculated values of the oxygen pressure for which the partial pressures of the various gaseous species are equal to 1 bar and 0.1 bar. For concentrated media (around 65%), the curves tend to deviate from a linear evolution; this phenomenon is due to the variation of the water vapor pressure.

The oxygen pressure is directly linked to the oxidizing power of the medium. Therefore, the curves relative to the different gases delimit the stability domain of nitric acid solutions in oxidation and in reduction under a pressure of 1 bar.

According to the diagrams at 25°C, as well as at 100°C, nitric acid should not be stable and should decompose into nitrogen and oxygen. In practice, the curves corresponding to the variation of the oxygen pressure for a pressure of 1 bar of nitrogen, N_2, and for a pressure of 1 bar of dinitrogen monoxide, N_2O, are found at much lower oxygen pressures than the values calculated. Literature results report that nitrogen and dinitrogen monoxide are formed at potentials lower than 0.7 V/NHE i.e. 0 V/SSE.[22] This potential gives a value of the oxygen pressure of log $(P_{O_2}) \approx -30$, which is much lower than the values obtained by calculations. This behavior is probably due to the slow kinetics of the reactions involving N_2 or N_2O.

If N_2 and N_2O are not considered, the curves relative to the gaseous nitrogen oxides, NO and NO_2, delimit the stability domain of nitric solutions when the medium is reduced (under a pressure of 1 bar). This domain is equivalent to the electroactivity domain for cathodic potentials in a Pourbaix diagram. In oxidation, the domain is limited by the formation of oxygen. In the diagram at 25°C, the reduction of nitric acid leads to the formation of NO for nitric acid concentrations lower than 60 wt-% ($P_{HNO3} = 1.58 \cdot 10^{-3}$ bar) and to the formation of N_2O_4 for higher concentrations. At 100°C, the electroactivity domain of nitric acid in reduction under a pressure of 1 bar is also divided into two parts. The formation of NO limits the stability domain of nitric acid for concentrations lower than 40 wt-% ($P_{HNO3} = 0.0115$ bar) and the formation of NO_2 limits the stability domain for higher concentrations.

The junction between the $[-\log(P_{HNO3})]$ scale and the pH scale is made with the dissociation constant of nitric acid. Consider the equilibrium:

$$HNO_{3(g)} \rightleftharpoons H^+_{(aq.)} + NO^-_{3(aq.)} \quad (4)$$

For pH = 0, the activity of protons is considered to be equal to its concentration, and the equilibrium constant of reaction (4), known in the literature,[18,19] can be written as:

$$K_{diss.} = \frac{[H^+][NO_3^-]}{P_{HNO_3}}$$

This expression leads to:

$$-\log(P_{HNO_3}) = 2\,pH + \log(K_{diss.})$$

Therefore the junction between pH and nitric acid vapor pressure can be established.

Incorporation of Experimental Measurements into the Calculated Diagram at 100°C

In Figure 5, the variation of the oxygen pressure for the various gaseous species is represented. Moreover, the variation of the oxygen pressure is drawn for a concentration of nitrous acid of 10^{-2} mol L^{-1}. To represent this variation, the mean experimental value of the free energy of formation of nitrous acid in a nitric acid solution at 100°C, $\Delta G_f(HNO_2) = -36.3 \pm 1$ kJ mol^{-1}, is used and the equilibrium (f) is considered:

$$HNO_{3(g)} \rightleftharpoons HNO_{2(aq.)} + \frac{1}{2} O_{2(g)}$$

Then, the variation of the oxygen pressure can be written as:

$$\log P_{O_2} = 2\log K_f + 2\log P_{HNO_2} - 2\log[HNO_2]$$

Here all the terms are known for a given nitric acid concentration and temperature. The experimental curve is represented with error bars corresponding to a potential measurement error of ± 5 mV [or 1 kJ mol^{-1} in terms of $\Delta G_f(HNO_2)$].

For pH > 0, the variations of the oxygen pressure, for a concentration of nitrous acid of 10^{-2} mol L^{-1}, obtained with literature values of $\Delta G_f^0(HNO_2)$, are also represented. The experimental variation is located between those curves.

An experimental potential scale, referenced to the saturated sulfate electrode at 25°C, has been superimposed on the $\log(P_{O2})$ scale for each nitric acid concentration. It is necessary to be aware that this experimental potential scale is not a thermodynamic scale because of the temperature gradient. The working electrode was in the nitric acid solution at 100°C and the reference electrode in a compartment of the electrochemical bridge at 25°C for practical considerations. However, all the measurements were performed in the same conditions and are reproducible, and can therefore be compared between with other.

The correspondence between the oxygen pressure and the potential scale is established in the following way. The potential can be expressed according to the system O_2/H_2O:

$$E = E^0_{O_2/H_2O} + \frac{RT}{2F}\ln\frac{P_{O_2}^{1/2}[H^+]^2}{P_{H_2O}}$$

For a given nitric acid concentration and temperature, the concentration of protons and the water vapor pressure are fixed. They can be included in an apparent standard potential, $E^{0'}{}_{O2/H2O}$, and the potential can be written as:

$$E = E^{0'}_{O_2/H_2O} + 2.303\frac{RT}{4F}\log P_{O_2}$$

For a variation of 1 of the $\log(P_{O2})$ scale for a given nitric acid concentration at 100°C, the apparent standard potential, $E^{0'}{}_{O2/H2O}$ is constant and the corresponding variation of the potential is equal to 18.5 mV according to:

$$\Delta E = 2.303\frac{RT}{4F} = 18.5\ \text{mV}$$

The electrochemical measurements led to the determination of the apparent standard potential of the HNO_3/NO_2 system, $E_2{}^{0'}$, at nitric acid concentrations of 4 mol L^{-1}, 8 mol L^{-1}, and 14.4 mol L^{-1}. Therefore, the values of $E_2{}^{0'}$ could be placed on the diagram, for each nitric acid concentration, on the curve representing the variation of the oxygen pressure for a nitrogen dioxide pressure of 1 bar.

At a given nitric acid concentration, knowing the value of $E_2{}^{0'}$, all the other potentials can be determined with the

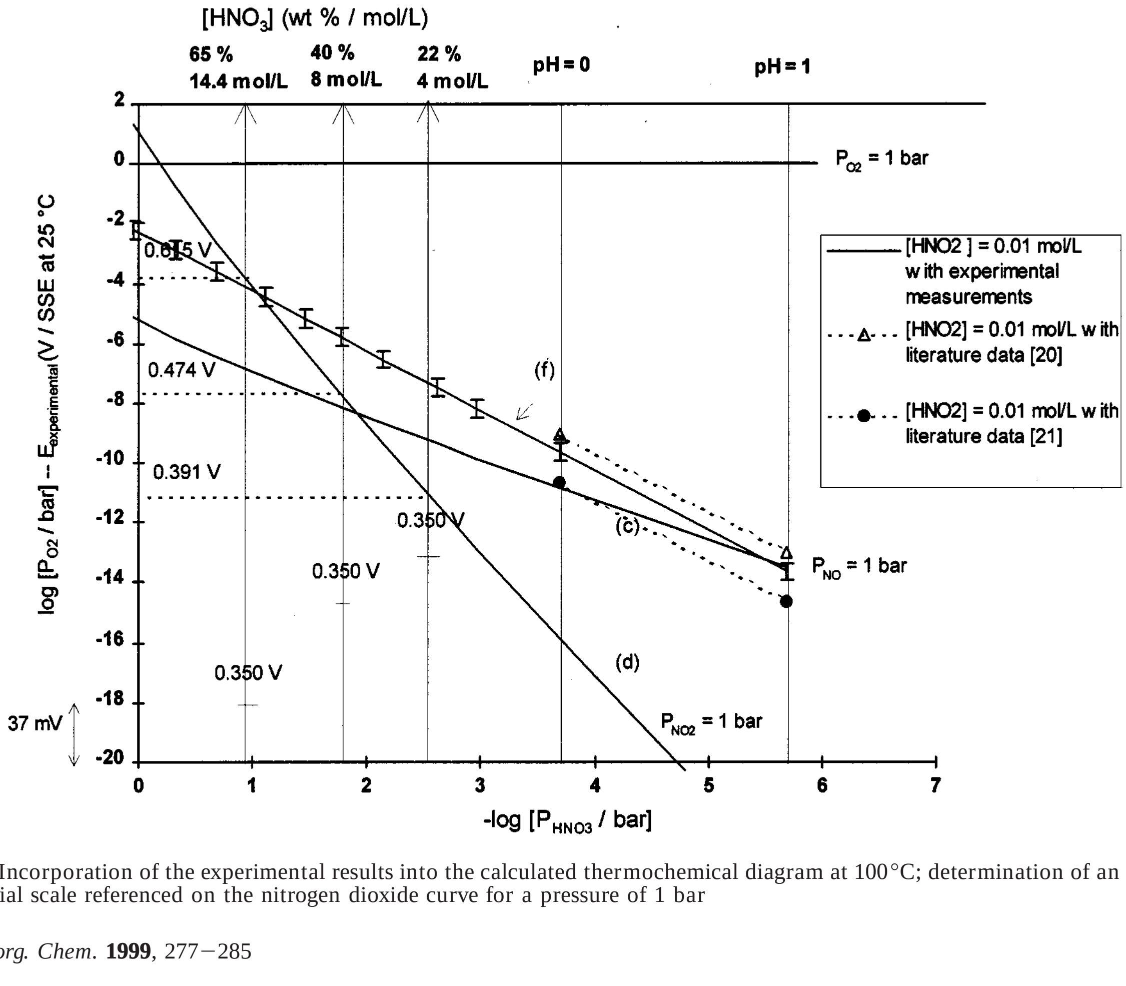

Figure 5. Incorporation of the experimental results into the calculated thermochemical diagram at 100°C; determination of an experimental potential scale referenced on the nitrogen dioxide curve for a pressure of 1 bar

correspondence between the log(P_{O2}) axis and the experimental potential axis.

In Figure 5, the potential value of 0.350 V/(SSE at 25°C) for the three nitric acid concentrations is represented in order to show the variation of the experimental potential scale with the nitric acid concentration. For each nitric acid concentration, an experimental potential scale has then been established. This scale allows any experimental measurement to be placed on the diagram.

Conclusion

The method used in this study to represent the nitric acid chemical properties can be extended to any concentrated medium. The choice of an x scale linked to a gaseous species avoids the use of uncertain data on the dissociation of concentrated acid and of thermochemical data of soluble species which are often unknown in the working medium. Moreover, working with vapor pressures in concentrated media allowed us to obtain a more expanded scale.

In the case of nitric acid, the major soluble species apart from nitric acid is nitrous acid. For this substance, uncertainties remained in the value of the Gibbs free energy of formation in solution at 100°C. Values of the free energy of formation of nitrous acid in solution have, however, now been determined experimentally for nitric acid concentrations varying from 4 mol L^{-1} to 14.4 mol L^{-1}. These values led to the determination of the free energy of formation of nitrous acid in solution for the whole nitric acid concentration range. Knowledge of this value allowed us to place the variation of the oxygen pressure for a concentration of nitrous acid of 10^{-2} mol L^{-1} into the diagram.

Finally, the major species found when nitric acid is reduced at potentials close to the equilibrium potential have been determined: NO for nitric acid concentration lower than 40% (ca. 8 mol L^{-1}) and NO_2 for higher concentrations. An experimental potential scale, referenced to the saturated mercurous sulfate electrode at 25°C, was also established with the experimental determination of the HNO_3/HNO_2 and HNO_3/NO_2 systems.

This representation appears to be a useful tool to understand and clarify the behavior of concentrated nitric acid. In the subsequent part of the study, corresponding to an electrokinetic investigation of the reduction of concentrated nitric acid at 100°C, this diagram will help us to understand reduction mechanisms of nitric acid occurring at a platinum electrode.

Experimental Section

Reactor Cell: The reactor was regulated at 100°C and contained 1 L of solution with the volume of the vapor phase approximately 0.6 L. The size of reactor was chosen for the measurements under a flow of nitrogen dioxide as a large volume of solution avoided a significant variation in the composition of the liquid medium with the gaseous flow. The working electrode was a platinum plate of 0.25 cm^2 polished to a mirror finish. The following circuit was set up for measuring the electrode potential: working electrode/HNO_3 solution, 100°C/HNO_3 solution, 25°C/saturated KNO_3 solution, 25°C/saturated K_2SO_4 solution, 25°C/saturated sulfate electrode, 25°C. The reference electrode was a saturated mercurous sulfate electrode and may be described as: Hg/Hg_2SO_4/saturated K_2SO_4 solution. The potential of this reference electrode relative to the standard hydrogen electrode at 25°C is equal to $E_{SSE} = 0.640$ V/SHE.[23] The difference in temperature between the working electrode and the reference electrode prevented us from measuring thermodynamic potentials: The potential scale established was not a thermodynamic scale but rather, was purely experimental allowing us to compare values obtained in the same conditions.

Electrochemical Apparatus and Procedure: The potential measurements were made with an EG&G PAR Model 273 potentiostat as other electrochemical experiments, which are not presented here, were performed in the same time. Measurements were performed in 22 wt-% (4 mol L^{-1}), 40 wt-% (8 mol L^{-1}), 48 wt-% (10 mol L^{-1}), and 65 wt-% (14.4 mol L^{-1}) nitric acid solutions at 100°C with addition of nitrites (nitrous acid in concentrated medium) in the solution or under a controlled atmosphere performed with a gas flow imposing a specific NO_2 pressure. The NO_2 flow was performed by combining air and NO at specific rates to form NO_2 at the desired pressures according to:

$$NO(g) + {}^{1}/_{2}\, O_2(g) \rightleftharpoons NO_2(g)$$

The NO_2 pressure was verified by bubbling NO_2 for one hour through a sodium hydroxide solution and measuring the concentration of nitrites as NO_2 reacts with NaOH to form nitrites according to:

$$2\, NO_2(g) + 2\, NaOH \rightleftharpoons NaNO_2(aq.) + NaNO_3(aq.) + H_2O$$

The concentration of nitrous acid (nitrite ions) in solution was measured by colorimetry with a Perkin−Elmer UV/Vis spectrometer according to the Griess method.[24]

Acknowledgments

The authors are grateful to COGEMA for their financial contribution. They also express thanks to the SGN company and CEA company for their interest in this work and their scientific contribution.

---

[1] M. Leduc, M. Pelras, J. Sannier, G. Turluer, R. Demay, “Etudes de corrosion sur les matériaux destinés aux usines de retraitement”, *RECOD'87*, paper 195, Paris, **1987**.

[2] P. Fauvet, G. Pinard Legry, “Corrosion aspects in reprocessing technology”, *EUROCORR'92*, Espoo, Finland, **1992**.

[3] J. P. Schosger, F. Dabosi, R. Demay, P. Fauvet, J. P. Moulin, G. Santarini, “Influence of corrosion products on the passivation of AISI 304 L stainless steel in nitric acid media”, *EUROCORR'96*, Nice, France, **1996**, session IX, paper 32.

[4] [4a] G. Picard, H. Lefebvre, B. Tremillon, *J. Electrochem. Soc.* **1987**, *134*, 52−58. − [4b] G. Picard, H. Lefebvre, B. Tremillon, *Molten Salts*, The Electrochemical Society Softbound Proceedings Series, **1987**, *vol. 87−7*, p. 1028−1042.

[5] M. Pourbaix, *Atlas d'équilibres électrochimiques*, Gauthier-Villars & Cie, Paris, **1963**, p. 493−503.

[6] W. Davis, H. J. de Bruin, *J. Inorg. Nucl. Chem.* **1964**, *26*, 1069−1083.

[7] A. Potier, *Ann. Faculté Sci. Univ. Toulouse Sci. Math. Sci. Phys.* **1956**, *20*, 1−98.

[8] R. Vandoni, M. Laudy, *J. Chem. Phys.* **1952**, *49*, 99−102.

[9] W. C. Sproesser, G. B. Taylor, *J. Am. Chem. Soc.* **1921**, *43*, 1782−1787.

[10] W. J. Hamer, Y-C. Wu, *J. Phys. Chem. Ref. Data* **1972**, *1*, 1047−1063.

[11] R. Haase, K. H. Dücker, H. A. Küppers, *Ber. Bunsenges. Phys. Chem*. **1965**, *69*, 97−109.
[12] R. Flatt, F. Benguerel, *Helv. Chim. Acta* **1962**, *45*, 1765−1772.
[13] M. A. Yakimov, V. Y. Mishin, *Sov. Radiochem*. **1964**, *6*, 523.
[14] J. L. Clavelin, P. Mirabel, *J. Chim. Phys*. **1979**, *76*, 533−537.
[15] T. Marnac, M. Enjalbert, *Chim. Ind. Genie Chim*. **1967**, *98*, 1047.
[16] I. Barin, *Thermochemical data of pure substances*, VCH Verlagsgesellschaft, Weinheim, **1993**.
[17] O. Knacke, O. Kubaschewski, K. Hesselmann, *Thermochemical properties of inorganic substances*, Springer-Verlag, Berlin, **1991**.
[18] S. E. Schwartz, W. H. White, *Adv. Environ. Sci. Eng*. **1981**, *4*, 1−45.
[19] H. C. Hegelson, *J. Phys. Chem*. **1967**, *71*, 3121−3136.
[20] H. E. Barner, R. V. Scheuerman, *Handbook of thermochemical data for compounds and aqueous species*, John Wiley & Sons, New York, **1978**.
[21] D. D. Wagman, Evans, Pauker, Schumm, Halow, Bailey, Churney, Nuttall, *J. Phys. Chem. Ref. Data* **1982**, *11*, 2.64−2.65.
[22] V. P. Razygraev, M. V. Lebedeva, S. A. Kabakchi, E. Yu. Ponomareva, R. S. Balovneva, L. P. Lobanova, *J. Appl. Chem. USSR* **1988**, *61*, 71−79.
[23] A. J. Bard, L. R. Faulkner, *Electrochimie: principes et applications*, Masson & Cie, Paris, **1983**, 785.
[24] G. Charlot, *Les méthodes de la chimie analytique − Analyse quantitative minérale*, Masson & Cie, Paris, **1961**, p. 620.

Received May 29, 1998
[I98170]